Advances in Nano Research, *Vol. 10, No. 4 (2021) 339-347*
DOI: https://doi.org/10.12989/anr.2021.10.4.339

One-dimensional Schottky nanodiode based on telescoping polyprismanes

Daulet Sergeyev*[1,2]

[1] *Department of Physics, K. Zhubanov Aktobe Regional State University, 34A Moldagulova avenue, 030000 Aktobe, Kazakhstan*
[2] *Department of Radio Electronics, T. Begeldinov Aktobe Avation Institute, 39 Moldagulova avenue, 030012 Aktobe, Kazakhstan*

(*Received July 18, 2020, Revised November 21, 2020, Accepted January 2, 2021*)

Abstract. In the framework of the density functional theory combined with the method of non-equilibrium Green functions (DFT + NEGF), the electric transport properties of a one-dimensional nanodevice consisting of telescoping polyprismanes with various types of electrical conductivity were studied. Its transmission spectra, density of state, current-voltage characteristic, and differential conductivity are determined. It was shown that $C_{[14,17]}$, $C_{[14,11]}$, $C_{[14,16]}$, $C_{[14,10]}$ show a metallic nature, and polyprismanes $C_{[14,5]}$, $C_{[14,4]}$ possess semiconductor properties and has a band gap of 0.4 eV and 0.6 eV, respectively. It was found that, when metal $C_{[14,11]}$, $C_{[14,10]}$ and semiconductor $C_{[14,5]}$, $C_{[14,4]}$ polyprismanes are coaxially connected, a Schottky barrier is formed and a weak diode effect is observed, i.e., manifested valve (rectifying) property of telescoping polyprismanes. The enhancement of this effect occurs in the nanodevices $C_{[14,17]} - C_{[14,11]} - C_{[14,5]}$ and $C_{[14,16]} - C_{[14,10]} - C_{[14,4]}$, which have the properties of nanodiode and back nanodiode, respectively. The simulation results can be useful in creating promising active one-dimensional elements of nanoelectronics.

Keywords: polyprisman; Schottky nanodiode; electron transport; current-voltage characteristic; differential conductivity

1. Introduction

Recently, an intensive search has been conducted for new materials and the study of their electrophysical properties, aimed at creating the active elements of modern nanoelectronics (Dragoman and Dragoman 2017, Murali 2012). Especially this problem has become urgent for obtaining nanomaterials with specified electrophysical characteristics for miniaturization of electronic components (Marani and Perri 2017, Agrait *et al*. 2003, Sergeyev and Zhanturina 2019), since the use of nanoscale electronic components provides huge savings in the consumption of electrical energy from power sources and it allows many times to reduce the size and weight of the equipment. The creation of such elements requires a theoretical and experimental study of the electric transport properties of individual molecules, which is of interest from the point of view of applied applications (Cuevas and Scheer 2017, Paul *et al*. 2014, Sergeyev 2020a). One of the promising nano objects for this purpose is one-dimensional (1D) nanostructures, such as nanotubes and nanowires, which have unusual electrophysical properties (Xiang *et al*. 2020, Kumar 2018, Sergeyev 2020b). In this regard, carbon nanotubes (CNTs) are primarily considered as promising materials for the development of nanoelectronic elements. The combination of various seamless or cross-connections built from CNTs with different types of conductivity forms a Schottky rectifying barrier. They are well suited to solve the problems of miniaturization of various electronic devices (Fuhrer *et al*. 2000). To miniaturize electronic devices, the transport properties of CNTs in the form of intramolecular contacts are especially widely studied (Wu *et al*. 2018).

A special type of single-walled nanotubes with a very small cross-section in the form of a regular polygon are prisman nanotubes – polyprismanes. [*n*, *m*] -polyprismanes are atomic rings stacked in layers, where *m* is the number of vertices of the ring, *n* is the number of layers. According to the estimate given in Maslov *et al*. (2020), the number of ballistic channels for polyprismanes increases with their effective diameter. The calculations were carried out using the density functional theory in the Quantum Espresso program. It turned out that metallic carbon $C_{[n, 7]}$- and $C_{[n, 8]}$ -polyprismanes have six ballistic channels. This means that they have a conductivity of $6G_0$ (here G_0 is the quantum of conductivity). It is assumed that the conductive properties of polyprismanes result from the hybridization of local atomic orbitals from various layers of the nanostructure into the global molecular orbital near the Fermi level. In this case, the electrons belonging to the molecular orbital that crosses the Fermi level become delocalized and participate in the appearance of conductivity. Note that the electronic conductivity near the Fermi energy of traditional metal CNTs is significantly lower than that of polyprismanes.

Recently, to create various nanodevices, telescoping multi-walled nanotubes connected by a van der Waals bond have found application. Such nanostructures are formed from CNT compounds by the electrical sharping technique (Cumings and Zettl 2000). In such systems, inter-shell interaction plays a key role in structural stability and electronic property (Pomorski *et al*. 2003). Note that inter-shell electron transport in telescoping CNTs is similar to electron transport through molecules in terms of the fact

*Corresponding author, Ph.D., Professor,
E-mail: serdau@mail.ru

ISSN: 2287-237X (Print), 2287-2388 (Online)

that both of them occur in a finite region (Pomorski *et al*. 2004). In work (Yan *et al*. 2006), such coaxial CNTs are used to develop a nanoswitch. It turned out that such switches are conveniently turned on or off using the relative movement of the pipes along the axis of the tube.

One of the active electronic components of nanoelectronics is nanodiodes. They are nanodevices capable of transmitting electric current in one direction. Currently, several options have been proposed for the implementation of nanodiodes based on various materials, for example, based on hybrid materials from organic and inorganic semiconductors (Pinto and Gonzalez 2006), based on the graphene–semiconductor interface (Lee *et al*. 2016), based on the metal–oxide (Lee *et al*. 2019) and others.

Note that at present, along with 1D Schottky nanodiodes, theoretical and experimental studies of two-dimensional (2D) nanodiodes are being intensively carried out (Wang *et al*. 2020). In paper (Liu *et al*. 2020), calculations were performed within the framework of the density functional theory, that demonstrate asymmetric electronic properties in the metal – semiconductor – metal interface, which consists of combinations of van der Waals heterostructures. Based on the calculation of the surface potential (using the 2D density of states in combination with the Fermi-Dirac distribution for the statistics of electrons and holes), a new analytical model has been developed to describe the current-voltage characteristics of field-effect transistors made of 2D materials with a Schottky barrier (Ahsan *et al*. 2020). In paper (Lan *et al*. 2020), it was shown from first principles that the electronic properties of graphene and $MoTe_2$ layers are well preserved in heterostructures due to weak van der Waals interlayer interaction, and the Fermi level moves towards the minimum of the conduction band of the $MoTe_2$ layer, forming a Schottky contact on the interface. Such 2D transition metal dichalcogenides with internally passivated surfaces are promising materials for the development of ultrathin optoelectronic devices. Schottky nanodiodes can be used to design rectifiers, logic elements, high-sensitivity sensors, etc. An interesting application of 2D Schottky nanodiodes for monitoring catalytic reactions and electronic control of chemical reactions is given in (Park and Somorjai 2020). A catalytic nanodiode, which is composed of a catalytic metal and semiconductor oxides forming a Schottky contact, is an important device for understanding the mechanism of catalytic reactions and developing a catalyst engineering structure. It allows you to directly measure the chemically induced hot electron flux and link it to catalytic activity (Lee *et al*. 2019). For example, using such nanodiode, consisting of an ultrathin aluminum film deposited on a semiconductor substrate, the kinetics of the aluminum – water reaction, which is a promising source for hydrogen production, can be monitored in real time (Nedrygailov *et al*. 2019). A key factor in evaluating catalytic activity is understanding the importance of the role of interfacial centers at the metal – oxide interfaces and the flow of hot electrons. To solve this problem, (Kim *et al*. 2020) presented a new design of catalytic nanodiodes, which uses as a 1D structure in the form of a nanosized Pt wire and a semiconductor substrate. In this design, a higher chemical current yield is observed compared to a 2D Pt-film/Si nanodiode. This is explained by a reduction in the path length of hot electrons at the edge of the Pt nanowires, which leads to a high probability of transport of hot electrons across the metal – oxide interface. Thus, nanosensors based on 1D Schottky nanodiodes have attracted attention due to their high sensitivity and speed. While Schottky contact nanowire sensors provide excellent performance in these areas, they can be further improved by a variety of techniques including defect engineering, surface modification, and the like (Meng and Li 2020).

In this paper, based on ab initio calculations, a model of a 1D nanodiode based on telescoping polyprismanes with different cross sections is proposed. Such nanodiodes can

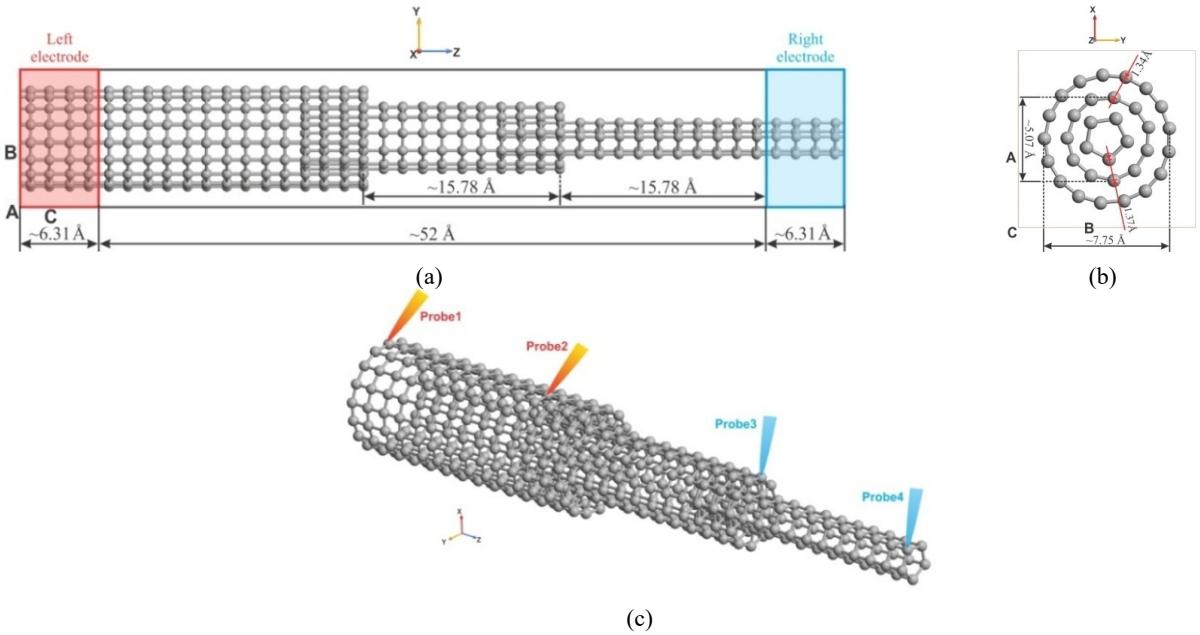

Fig. 1 The geometry of a 1D nanodiode based on telescoping polyprismanes $C_{[14,17]} – C_{[14,11]} – C_{[14,5]}$

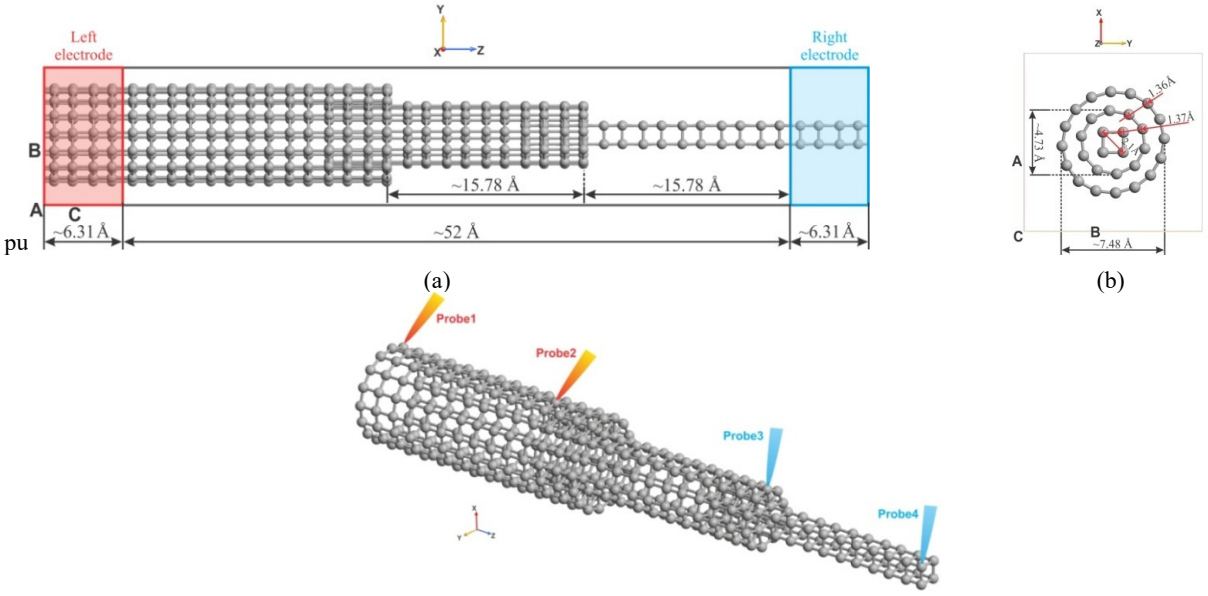

Fig. 2 The geometry of a 1D back nanodiode based on telescoping polyprismanes $C_{[14,16]} - C_{[14,10]} - C_{[14,4]}$

Table 1 The geometrical parameters of carbon [14, *m*] polyprismanes

m	4	5	10	11	16	17
$l_{\parallel}$, Å	1.4811	1.5759	1.4998	1.5030	1.4867	1.6146
$l_{\perp}$, Å	1.4811	1.5754	1.4515	1.4146	1.4532	1.4282
D, Å	2.0942	2.5499	4.7197	5.0741	7.4740	7.7452

be a fundamental building block for various nanodevices. For example, based on them, molecular rectifiers, logic elements, low-power ultra-sensitive sensors and others can be developed.

2. The geometry of telescoping polyprismanes

The geometry of the studied nanodevices, consisting of telescoping polyprismanes with different sections (diameters), is shown in Figs. 1 and 2. In the work, we limited ourselves to the use of polyprismanes, consisting of 11 layers of prismanes, with a length of ~ 20.42 Å. Electrodes were obtained by expanding the closing nanotubes along the C axis by ~ 6.31 Å. Two types of nanosystems with the same length but with different sections of telescoping nanotubes were considered: the first nanosystem consists of a combination of polyprismanes with odd numbers of rings $C_{[14,17]} - C_{[14,11]} - C_{[14,5]}$ (Fig. 1), and the second with even numbers of rings $C_{[14,16]} - C_{[14,10]} - C_{[14,4]}$ (Fig. 2). The distance between the electrodes is ~ 52 Å, where the central region of the $C_{[14,17]} - C_{[14,11]} - C_{[14,5]}$ and $C_{[14,16]} - C_{[14,10]} - C_{[14,4]}$ nanosystems is located, consisting of 462 and 420 carbon atoms, respectively. The distance between polyprismane tubes varies from 1.34 Å to 1.37 Å (Figs. 1(b), 2(b)).

The geometry optimization procedure for the nanostructures under consideration and the interatomic interaction description were carried out in the framework of the density functional theory (DFT), and the generalized gradient approximation GGA-PBE (Perdew *et al*. 1996, Ferre *et al*. 2016) was used as the exchange-correlation functional allows to accuratelydescribe similar structures. In the optimization of nanotubes, the distance between the atoms is completely weakened until the forces on the atoms of the molecule become less than 0.02 eV/Å. The main parameters of polyprismanes are given in Table 1 and in Figs. 1 and 2. In Figs. 1(c) and 2(c), points (Probe 1, 2, 3, 4) are marked for measuring the electrical parameters of nanodevices. (Hereinafter, when describing the calculated electrical parameters of nanotubes between the indicated points, for convenience we will use the term “measurement”.)

Fig. 3 shows the electron densities of the considered nanodiodes. As can be seen, the electron density at the junction of polyprismanes with different cross sections prevails over single-walled tubes. Obviously, this is the contribution of electrons of various layers of the nanostructure. The electron density at the intersection of C_{17} and C_{11} polyprismanes is ~ 525 $Å^{-3}$, and at the junction of C_{11} and C_5 is ~ 290 $Å^{-3}$ (Fig. 3(a)). For the considered polyprismanes with even numbers of atoms in the ring, the electron density is slightly lower: for C_{16} and C_{10} is ~ 470 $Å^{-3}$, and for C_{10} and C_4 is ~ 250 $Å^{-3}$ (Fig. 3(b)).

3. Main equations

Computer simulation of the electrical characteristics of a nanostructure was carried out within the framework of the density functional theory using the Non-Equilibrium Green's Functions (NEGF) method in the local density approximation (LDA) (Smidstrup *et al*. 2017, Stokbro 2008, Li *et al*. 2007). The simulation of the quantum transport characteristics of a nanostructure is implemented in the

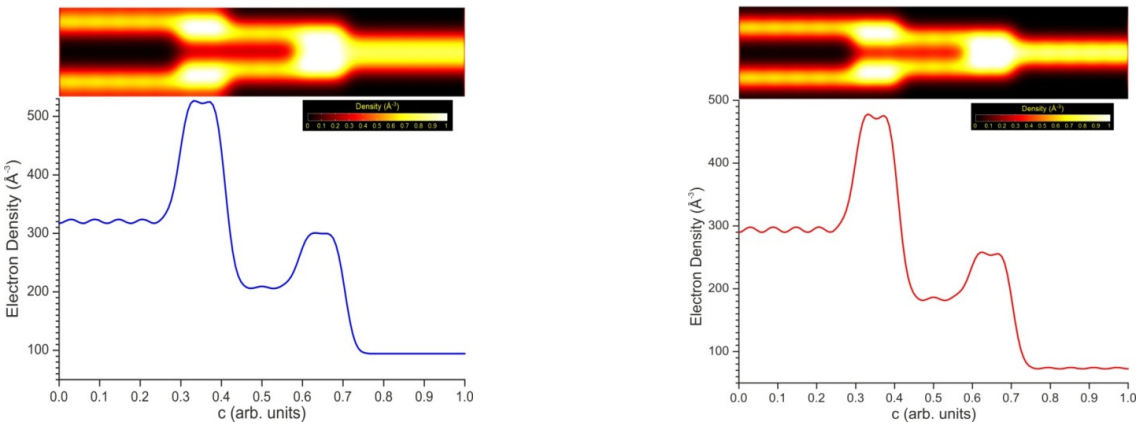

(a) (b)

Fig. 3 Electronic densities of nanodiodes based on $C_{[14,17]} – C_{[14,11]} – C_{[14,5]}$ (a) and $C_{[14,16]} – C_{[14,10]} – C_{[14,4]}$ (b)

Atomistix ToolKit with Virtual NanoLab program (Smidstrup *et al*. 2020). (A detailed description of the basic equations of this method is given in (Sergeyev and Shunkeyev 2018, Sergeyev 2020c)). To calculate the current-voltage characteristic (CVC) and differential conductivity, the transmission spectrum (function) of the considered nanodevice is first determined

$$T(\varepsilon) = tr[\Gamma^L G \Gamma^R G^\dagger] = tr[\Gamma^R G \Gamma^L G^\dagger], \quad (1)$$

where $\Gamma^{L(R)}(\varepsilon)$ is the broadening matrix (broadening function) of the left (right) electrode, $G(\varepsilon)$, $G^\dagger(\varepsilon)$ are the retarded and advanced Green functions, ε is the energy. The CVC of a nanostructure is calculated on the basis of the well-known Landauer equation, which indicates the fundamental relationship of electric current with the transmission spectrum (Landauer 1970)

$$I(V_L, V_R, T_L, T_R) = \frac{2e}{h}\int_{-\infty}^{+\infty} T(\varepsilon)\left[f\left(\frac{\varepsilon-\mu_R}{k_B T_R}\right) - f\left(\frac{\varepsilon-\mu_L}{k_B T_L}\right)\right] d\varepsilon, \quad (2)$$

where e is the electron charge, h is the Planck constant, $f(\varepsilon)$ is the Fermi energy distribution function of quasiparticles, k_B is the Boltzmann constant, T_R, T_L are the current temperatures of the left and right electrodes and μ_R, μ_L are the electrochemical potentials of the right and left electrodes.

The differential conductivity of telescoping prism nanotubes was obtained by calculating a self-consistent current for a number of applied biases and performing numerical differentiation

$$\sigma(V_{bias}, T_L, T_R) = \frac{I(V^1_{bias}, T_L, T_R) - I(V^2_{bias}, T_L, T_R)}{V^1_{bias} - V^2_{bias}}. \quad (3)$$

To determine the density of state (DOS) of telescoping nanotubes, we first calculate its local density of states (LDOS)

$$D(\varepsilon, r) = \sum_{ij} \rho_{ij}(\varepsilon)\phi_i(r)\phi_j(r), \quad (4)$$

where $\rho(\varepsilon) = \rho^L(\varepsilon) + \rho^R(\varepsilon)$, $\phi(r)$ is the basis orbital. The DOS of telescoping nanotubes is obtained by integrating LDOS over the entire space

$$D(\varepsilon) = \int drD(\varepsilon) = \sum_{ij} \rho_{ij}(\varepsilon)S_{ij}, \quad (5)$$

where $S_{ij} = \int \phi_i(r)\,\phi_j(r)dr$ is the overlap matrix.

4. Results and discussion

The evolution of the transmission spectrum of polyprisman nanodevices with an increase in bias voltage from -2 V to 2 V is shown in Figs. 4 and 5. The bias voltage increased with a step of 0.2 V. The transmission spectrum of polyprismanes uses the molecular orbit energies for the applied bias voltages to determine at which energies the electron transport will be the strongest. The spectra were built for the HOMO (Highest Occupied Molecular Orbital) – LUMO (Lowest Unoccupied Molecular Orbital) energies relative to the Fermi level energy, which was considered as zero energy ($\boldsymbol{\varepsilon_F = 0}$). In Fig. 2 different colored fills show various applied voltages (from black (-2 V) to army green (2 V)).

With an increase in the bias voltage, the intensity of the transmission spectrum also increases. It is known that the greater the number of peaks in the transmission spectrum, the higher the indices of the transport of quasiparticles through the nanodevice under consideration. At negative energy, the intensity of the transmission spectrum prevails relative to the intensity at positive energy. The transmission spectrum of coaxial polyprismanes $C_{[14,17]} – C_{[14,11]}$ shows that only near the Fermi energy does conductivity appreciably decrease. The combined polyprismanes $C_{[14,11]} – C_{[14,5]}$ in the energy range of -0.7 ÷ 2 eV do not pass quasiparticles, forming a HOMO–LUMO gap of 2.7 eV. When forming from these tubes the nanodevice $C_{[14,17]} – C_{[14,11]} – C_{[14,5]}$ the HOMO–LUMO gap width remains the same 2.7 eV, however, a slight shift towards positive energy is observed (-0.5 ÷ 2.2 eV), and a series of peak resonant structures appears at positive energy.

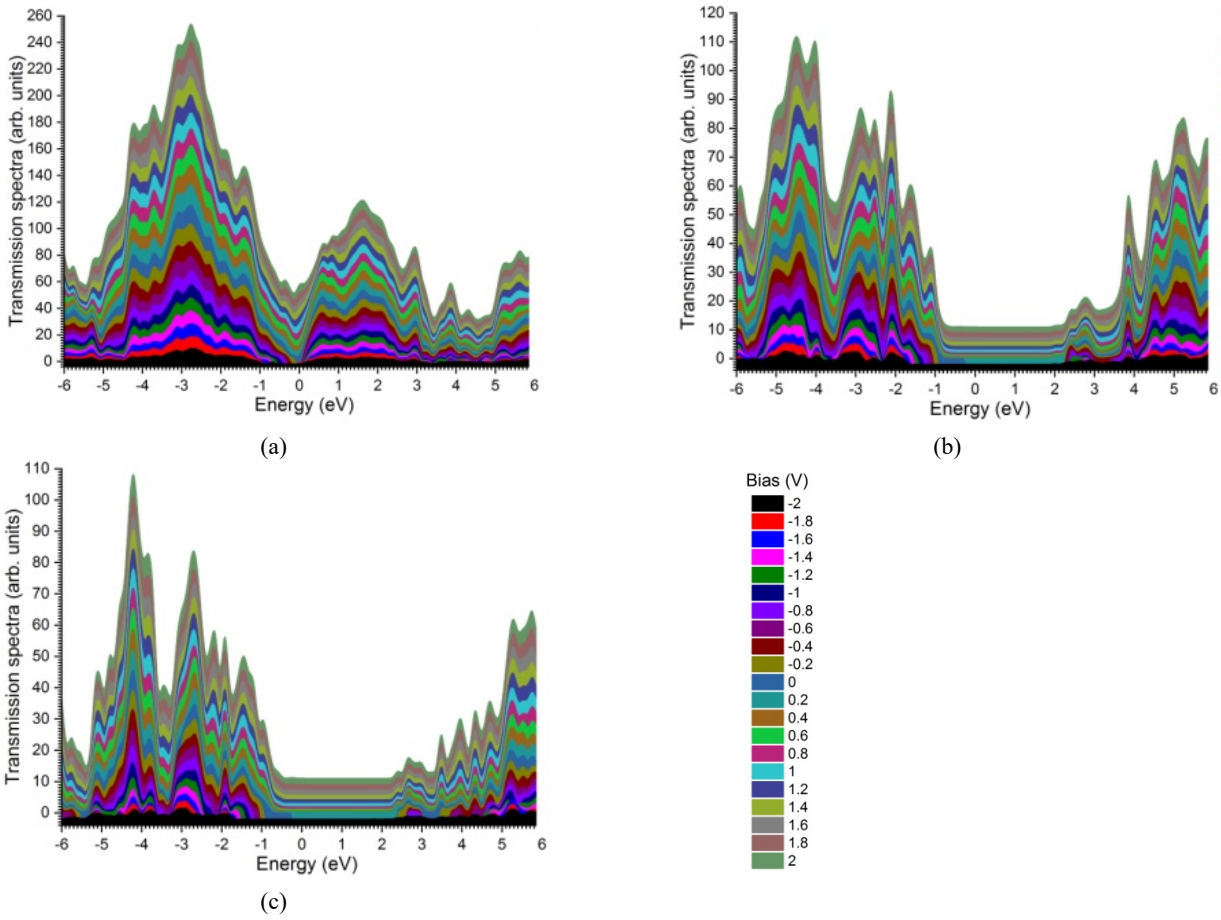

Fig. 4 Transmission spectra of nanodevice $C_{[14,17]} - C_{[14,11]} - C_{[14,5]}$:
(a) $C_{[14,17]} - C_{[14,11]}$; (b) $C_{[14,11]} - C_{[14,5]}$; (c) $C_{[14,17]} - C_{[14,11]} - C_{[14,5]}$

Noticeable changes relative to previous nanoobjects are observed in the transmission spectrum of nanodevices from polyprismanes $C_{[14,16]}$, $C_{[14,10]}$, $C_{[14,4]}$ (Fig. 5). As can be seen, the polyprisman structures from $C_{[14,16]} - C_{[14,10]}$ have good conductivity. Combined $C_{[14,10]} - C_{[14,4]}$ nanotubes in the range of -1.8 ÷ 3.9 eV do not pass quasiparticles, a wide HOMO–LUMO gap of 5.7 eV is formed. During the formation of the coaxial structure $C_{[14,16]} - C_{[14,10]} - C_{[14,4]}$, the gap remains.

The simulation results of the CVC and differential conductivity of $C_{[14,17]} - C_{[14,11]} - C_{[14,5]}$ nanodevices are shown in Fig. 6. (CVC and differential conductivity of the nanostructures under consideration were calculated using equations (2, 3)). On CVC "measured" between points (Probe) 1 and 3 ($C_{[14,17]} - C_{[14,11]}$) step sections appear in the form of "Coulomb staircases" observed in single-electron devices (Schönenberger *et al*. 1993, Kiguchi 2016). However, unlike single-electron devices, these step structures on the CVC of a nanodevice do not appear periodically. Typically, Coulomb staircases are clearly observed as oscillations with a constant voltage period in the *dI*/*dV*-spectrum. In this case, peak structures occur at bias voltages of -1.7 V, -1.13 V, -0.68 V, 0.16 V, 0.46 V, 0.9 V, 1.73 V and their frequency by voltage is not saved. Nevertheless, we believe that the nature of these features of the CVC between points 1 and 3 is related to the Coulomb interaction of quasiparticles in polyprismanes $C_{[14,17]}$ and $C_{[14,11]}$, since the study of similar parameters of polyprismanes $C_{[14,16]} - C_{[14,10]}$, given below, indicates the dominance of the Coulomb effect in these nanostructures.

The current $I_{2\text{-}4}$ between points 2 and 4 in the voltage range from -2 V to 0.83 V is zero, i.e. a nanodevice from $C_{[14,11]} - C_{[14,5]}$ of polyprismanes does not pass current at a negative bias voltage (Fig. 6(a), curve 1). This is due to the fact that a Schottky rectifying barrier is formed between metallic $C_{[14,11]}$ and semiconductor $C_{[14,5]}$ polyprisman. This property of the nanostructure could be used for the development of nanodiodes, however, the current flowing through the structure at a positive voltage of 0.83 ÷ 2 V is negligible, the maximum current is only 350 nA at a voltage of 1.42 V. The current value at a positive voltage in 25 times increases in the case of a coaxial connection of the three considered polyprismanes. The current $I_{1\text{-}4}$, measured between points 1 and 4 is 9 μA (Fig. 6(a), curve 3). In this case, in the voltage range of -2 ÷ 0.9 V, the nanodevice does not pass current and the previously observed diode effect is preserved. On the *dI*/*dV* - spectrum of the nanodiode from $C_{[14,17]} - C_{[14,11]} - C_{[14,5]}$ polyprismanes two peaks of 128 mS, 206 mS at a voltage of 1.28 V and 1.73 V, respectively are clearly observed (Fig. 6b, curve 3). As can be seen, the structure of the peak of the *dI*/*dV*-spectrum at 1.73 V is preserved and is a copy of the $C_{[14,17]} - C_{[14,11]}$ polyprismanes peak, and the peak value at 1.28 V increased from 3 μS ($C_{[14,11]} - C_{[14,5]}$) up to 128 mS.

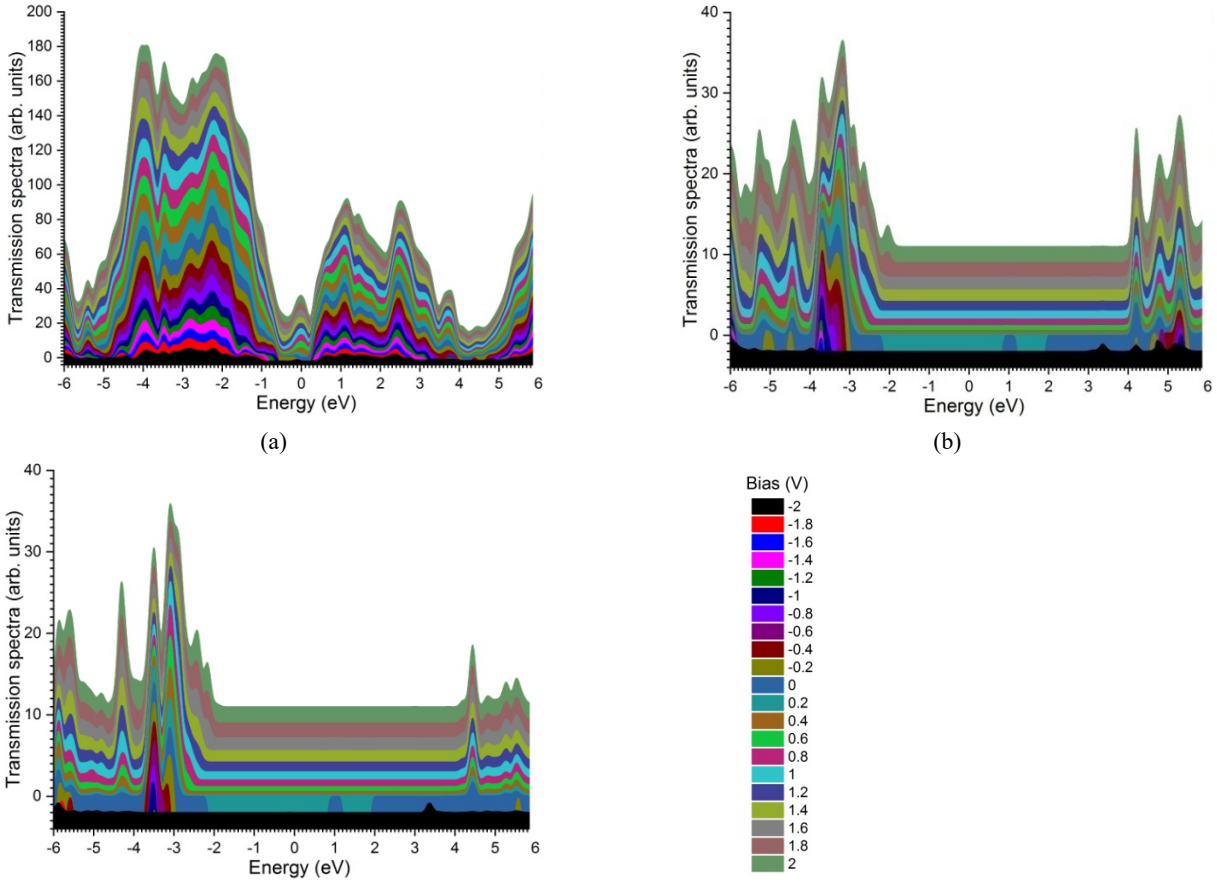

Fig. 5 Transmission spectra of nanodevice $C_{[14,16]} – C_{[14,10]} – C_{[14,4]}$:
(a) $C_{[14,16]} – C_{[14,10]}$; (b) $C_{[14,10]} – C_{[14,4]}$; (c) $C_{[14,16]} – C_{[14,10]} – C_{[14,4]}$

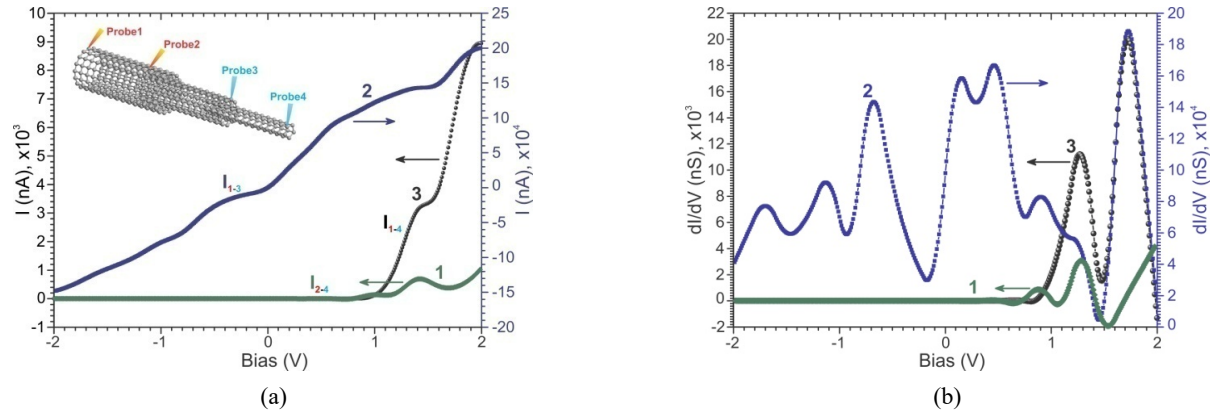

Fig. 6 IV- (a) and dI/dV-characteristics (b) of $C_{[14,17]} – C_{[14,11]} – C_{[14,5]}$ nanodevices: 1 – between points 2 and 4 (green curve); 2 – between points 1 and 3 (blue curve); 3 – between points 1 and 4 (black curve). Current indices show between which points they are measured

The electrical characteristics of the second nanoobject, consisting of a combination of polyprismanes $C_{[14,16]}$, $C_{[14,10]}$, $C_{[14,4]}$, are presented in Fig. 7. Apparently, they have other (opposite) electrical characteristics. On CVC "measured" between points (Probe) 1 and 3 ($C_{[14,16]} – C_{[14,10]}$), as in the previous object, distinct steps of Coulomb origin appear (Fig. 7(a), curve 2), since on the *dI*/*dV*-spectrum these Coulomb features manifest themselves in the form of quasiperiodic oscillations every ΔV. The averaged value $\Delta V \sim 0.7$ V. Then it is reasonable to assume that the appearance of oscillations in the *dI*/*dV*-spectrum (the appearance of step structures on the IV-characteristic) with a quasi-constant voltage period is associated with the effect of the Coulomb blockade (Grabert and Devoret 1992). Note that with a positive bias voltage on the CVC, the steps appear more often than with a negative voltage. The peak structures of differential conductivity are almost equivalent, their values vary from 9 μS to 12 nS. Dips in the

dI/dV-spectrum occur at voltages of -1.68 V, -1.11 V, 0.2 V, 0.8 V and 1.67 V. At a voltage of -1.68 V, negative differential conductivity is observed (Fig. 7(b), curve 2).

The current value $I_{2\text{-}4}$ (between points 2 and 4) in the voltage range from -1.2 V to 2 V is zero, which means the combination of polyprismanes from $C_{[14,11]} - C_{[14,5]}$ does not pass current with a positive voltage bias (Fig. 7(a), curve 1). This electrical property of the nanostructure is the opposite of the property of $C_{[14,11]} - C_{[14,5]}$ tubes. The maximum value of the transmitted current is only -55 nA (with V_{bias} = -2V). The current modulus at negative voltage increases to 115 nA in the coaxial structure of the three considered polyprismanes $C_{[14,16]}$, $C_{[14,10]}$, $C_{[14,4]}$. (Measurement of electrical characteristics between points 1 and 4 in Fig. 7). In this case, the valve property of the device is saved. This allows in the future to create a back nanodiode based on them. However, it should be noted that a sharp drop in current is observed in the CVC of the nano-object under consideration in the voltage range of -1.8 ÷ 1.6 V, forming a section of negative differential resistance. This results in the tunneling of quasiparticles in the indicated V_{bias} interval. At the *dI/dV*- characteristic at V_{bias} = -1.68 V, a negative differential conductivity of -140 nS is observed (Fig. 7, curve 3). The threshold voltage for turning on the back nanodiode is -0.8 V.

Fig. 8 presents the results of the calculation of the DOS of polyprismanes $C_{[14,17]}$, $C_{[14,11]}$, $C_{[14,5]}$, $C_{[14,16]}$, $C_{[14,10]}$, $C_{[14,4]}$. As can be seen, polyprismanes $C_{[14,17]}$, $C_{[14,11]}$, $C_{[14,16]}$, $C_{[14,10]}$ show a metallic nature. This statement is consistent with the results of (Katin *et al*. 2020), where it was established that carbon polyprismanes have a metallic nature only at a certain critical diameter, not less than ~ 3.5 Å. Polyprismanes $C_{[14,5]}$, $C_{[14,4]}$ have a band gap of 0.4 eV and 0.6 eV, respectively. This means that as the diameter increases, carbon polyprisman undergoes a change in electronic properties that strongly affect their electrical conductivity. Therefore, the connected polyprismanes $C_{[14,17]} - C_{[14,11]}$ and $C_{[14,16]} - C_{[14,10]}$ with metallic properties have good conductivity (see Figs. 6 and 7, curve 2). The connection of metal polyprismanes $C_{[14,11]}$, $C_{[14,10]]}$ with semiconductor $C_{[14,5]}$, $C_{[14,4]}$ will lead to a deterioration in conductivity, but weak valve properties appear (the ability of a nanodiode to pass current to one direction). Further, when connecting to the construction of nanodevices $C_{[14,11]} - C_{[14,5]}$, $C_{[14,10]} - C_{[14,4]}$ polyprismanes of $C_{[14,17]}$, $C_{[14,16]}$, accordingly, the rectifying effect of nanodiodes is enhanced.

5. Conclusions

Thus, in the framework of the theory of functional density, in this work, we studied the electrotransport

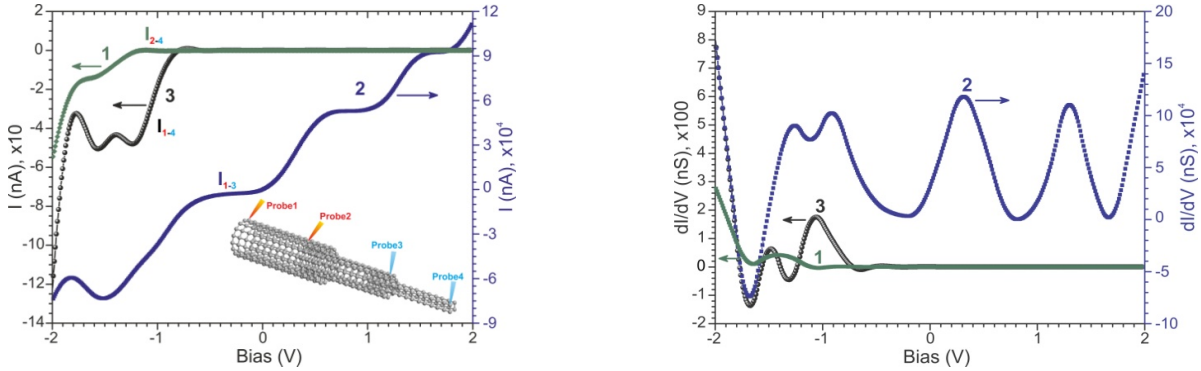

(a) (b)

Fig. 7 IV- (a) and dI/dV-characteristics (b) of $C_{[14,16]} - C_{[14,10]} - C_{[14,4]}$ nanodevice: 1 – between points 2 and 4 (green curve); 2 – between points 1 and 3 (blue curve); 3 – between points 1 and 4 (black curve). Indices of currents shows between which points they are measured

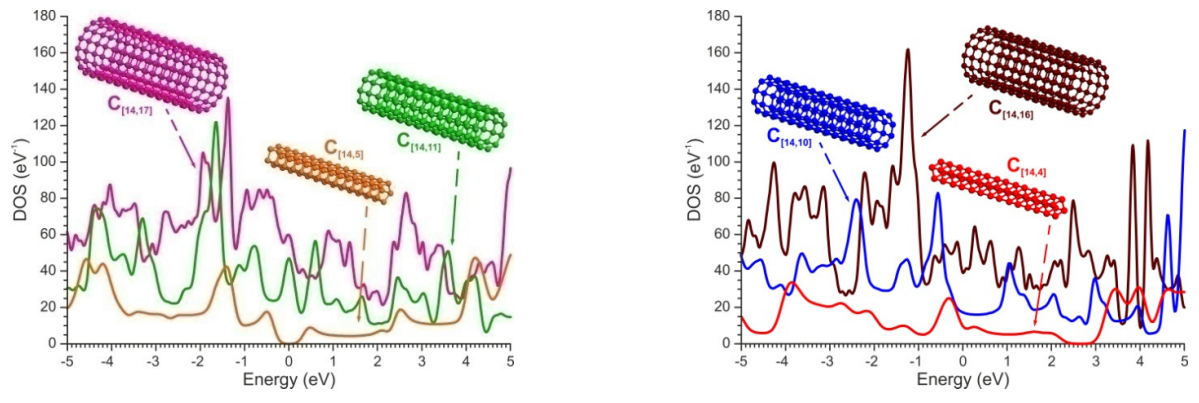

(a) (b)

Fig. 8 The density of states of prisman nanotubes: (a) $C_{[14,17]}$, $C_{[14,11]}$, $C_{[14,5]}$; (b) $C_{[14,16]}$, $C_{[14,10]}$, $C_{[14,4]}$

properties (transmission spectra, CVC, differential conductivity, electron density) of telescoping prisman nanotubes $C_{[14,17]} - C_{[14,11]} - C_{[14,5]}$ and $C_{[14,16]} - C_{[14,10]} - C_{[14,4]}$. It is shown that the combination of polyprismanes in the form of telescoping nanotubes with different cross sections leads to a significant change in their electrical properties. The following results were obtained:

- In the range of -0.5 ÷ 2.2 eV, a HOMO–LUMO gap is formed in the transmission spectrum of telescoping polyprismanes $C_{[14,11]} - C_{[14,5]}$, its width is 2.7 eV. The HOMO–LUMO gap of 5.7 eV is also observed in the spectrum of the polyprisman device $C_{[14,16]} - C_{[14,10]} - C_{[14,4]}$.
- On the CVC of polyprismanes $C_{[14,17]} - C_{[14,11]}$ and $C_{[14,16]} - C_{[14,10]}$, stepped sections appear in the form of "Coulomb staircases" observed in single-electron devices. We believe that these steps arise as a result of the Coulomb blockade effect.
- When polyprismanes are connected with different types of electrical conductivity, $C_{[14,11]} - C_{[14,5]}$ and $C_{[14,10]} - C_{[14,4]}$, a Schottky barrier is formed and a diode effect is observed.
- Polyprisman devices $C_{[14,17]} - C_{[14,11]} - C_{[14,5]}$ in the voltage range of -2÷0.9 V (with a negative bias voltage) does not pass electric current, i.e. possesses the properties of a nanodiode.
- Polyprisman devices $C_{[14,16]} - C_{[14,10]} - C_{[14,4]}$ in the voltage range of -0.8÷2 V (with a positive bias voltage) does not pass electric current, i.e. has the properties of a back nanodiode.
- The polyprismanes $C_{[14,17]}$, $C_{[14,11]}$, $C_{[14,16]}$, $C_{[14,10]}$ studied in this work exhibit a metallic nature, and the polyprismanes $C_{[14,5]}$, $C_{[14,4]}$ have semiconductor properties and have a band gap of 0.4 eV and 0.6 eV, respectively.

The knowledge of the features of the electrical properties of telescoping prismatic nanotubes presented in this work is very important for the development of high-performance nanoelectronic devices, and can serve as a valuable guide for the creation of Schottky nanodiodes.

Acknowledgments

This research has is funded by the Science Committee of the Ministry of Education and Science of the Republic of Kazakhstan (Grant No. AP08052562)

References

Agrait, N., Yeyati, A.L. and van Ruitenbeek, J.M. (2003), "Quantum properties of atomic-sized conductors", *Phys. Rep.*, **377**, 81-279. https://doi.org/10.1016/S0370-1573(02)00633-6

Ahsan, S.A., Singh, S.K., Yadav, C., Marin, E.G., Kloes, A. and Schwarz, M. (2020), "A Comprehensive Physics-Based Current-Voltage SPICE Compact Model for 2-D-Material-Based Top-Contact Bottom-Gated Schottky-Barrier FETs", *IEEE Transact. Electron Dev.*, **67**, 5188-5195. https://doi.org/10.1109/TED.2020.3020900

Cuevas, J.C. and Scheer, E. (2017), *Molecular Electronics* (*An Introduction to Theory and Experiment*), (2nd Edition), World Scientific Publishing Co. Pte. Ltd., Hackensack, NJ, USA.

Cumings, J. and Zettl, A. (2000), "Low-Friction Nanoscale Linear Bearing Realized from Multiwall Carbon Nanotubes", *Science*, **289**(5479), 602-604. https://doi.org/10.1126/science.289.5479.602

Dragoman, M. and Dragoman, D. (2017), *2D Nanoelectronics*: *Physics and Devices of Atomically Thin Materials*, Springer International Publishing, Cham, Switzerland. https://doi.org/10.1007/978-3-319-48437-2

Ferre, N., Filatov, M. and Huix-Rotllant, M. (eds.) (2016), *Density-Functional Methods for Excited States*, Springer International Publishing, Cham, Switzerland. https://doi.org/10.1007/978-3-319-22081-9

Fuhrer, M.S., Nygård, J., Shih, L., Forero, M., Yoon, Y.G., Choi, H.J., Ihm, J., Louie, S.G., Zettl, A. and McEuen, P.L. (2000), "Crossed nanotube junctions", *Science*, **288**, 494-497. https://doi.org/10.1126/science.288.5465.494

Grabert, H. and Devoret, M.H. (Eds.) (1992), *Single Charge Tunneling Coulomb Blockade Phenomena in Nanostructures*, Springer Science + Business Media, NY, USA. https://doi.org/10.1007/978-1-4757-2166-9

Katin, K.P., Grishakov, K.S., Gimaldinova, M.A. and Maslov, M.M. (2020), "Silicon rebirth: Ab initio prediction of metallic sp^3-hybridized silicon allotropes", *Computat. Mater. Sci.*, **174**, 109480. https://doi.org/10.1016/j.commatsci.2019.109480

Kiguchi, M. (Ed.) (2016), *Single-Molecule Electronics*: *An Introduction to Synthesis*, *Measurement and Theory*, Springer Science + Business Media, Singapore. https://doi.org/10.1007/978-981-10-0724-8

Kim, H., Kim, Y.J., Jung, Y.S. and Park, J.Y. (2020), "Enhanced flux of chemically induced hot electrons on a Pt nanowire/Si nanodiode during decomposition of hydrogen peroxide", *Nanoscale Adv.*, **2**, 4410-4416. https://doi.org/10.1039/d0na00602e

Kumar, B.R. (2018), "Investigation on mechanical vibration of double-walled carbon nanotubes with inter-tube Van der waals forces", *Adv. Nano Res., Int. J.*, **6**(2), 135-145. https://doi.org/10.12989/anr.2018.6.2.135

Lan, Y., Xia L.-X., Huang, T., Xu, W., Huang, G.-F., Hu, W. and Huang, W.-Q. (2020), "Strain and Electric Field Controllable Schottky Barriers and Contact Types in Graphene-$MoTe_2$ van der Waals Heterostructure", *Nanoscale Res. Lett.*, **15**, 180. https://doi.org/10.1186/s11671-020-03409-7

Landauer, R. (1970), "Electrical resistance of disordered one-dimensional lattices", *Philosoph. Mag.*, **21**(172), 863-867. http://dx.doi.org/10.1080/14786437008238472

Lee, Y.K., Choi, H., Lee, H., Lee, C., Choi, J.S., Choi, C.-G., Hwang, E. and Park, J.Y. (2016), "Hot carrier multiplication on graphene/TiO_2 Schottky nanodiodes", *Scientific Reports*, **6**, 27549. https://doi.org/10.1038/srep27549

Lee, H., Yoon, S., Jo, J., Jeon, B., Hyeon, T., An, K. and Park, J.Y. (2019), "Enhanced hot electron generation by inverse metal–oxide interfaces on catalytic nanodiode", *Faraday Discuss.*, **214**, 353-364. https://doi.org/10.1039/C8FD00136G

Li, R., Zhang, J., Hou, S., Qian, Z., Shen, Z., Zhao, X. and Xue, Z. (2007), "A corrected NEGF + DFT approach for calculating electronic transport through molecular devices: Filling bound states and patching the non-equilibrium integration", *Chem. Phys.*, **336**, 127-135. https://doi.org/10.1016/j.chemphys.2007.06.011

Liu, J., Ren, J.-C., Shen, T., Liu, X., Butch, C.J., Li, S. and Liu, W. (2020), "Asymmetric Schottky Contacts in van der Waals Metal-Semiconductor-Metal Structures Based on Two-Dimensional Janus Materials", *Research*, **2020**, 6727524. https://doi.org/10.34133/2020/6727524

Marani, R. and Perri, A.G. (2017), "An approach to model the temperature effects on I-V characteristics of CNTFETs", *Adv. Nano Res., Int. J.*, **5**(1), 61-67. https://doi.org/10.12989/anr.2017.5.1.061

Maslov, M.M., Grishakov, K.S., Gimaldinova, M.A. and Katin, K.P. (2020), "Carbon vs silicon polyprismanes: a comparative study of metallic sp^3-hybridized allotropes", *Fuller. Nanotub. Carbon Nanostruct.*, **28**(2), 97-103. https://doi.org/10.1080/1536383X.2019.1680974

Meng, J. and Li, Z. (2020), "Schottky-Contacted Nanowire Sensors", *Adv. Mater.*, 2000130. https://doi.org/10.1002/adma.202000130

Murali, R. (Ed.) (2012), *Graphene Nanoelectronics: From Materials to Circuits*, Springer, NY, USA. https://doi.org/10.1007/978-1-4614-0548-1

Nedrygailov, I.I., Heo, Y., Kim, H. and Park, J.Y. (2019), "Charge Transfer during the Aluminum−Water Reaction Studied with Schottky Nanodiode Sensors", *ACS Omega*, **4**, 20838-20843. https://doi.org/10.1021/acsomega.9b03397

Park, Y.J. and Somorjai, G.A. (2020), "Nanodiode-based hot electrons: Influence on surface chemistry and catalytic reactions", *MRS Bulletin*, **45**, 26-31. https://doi.org/10.1557/mrs.2019.295

Paul, W., Oliver, D. and Grutter, P. (2014), "Indentation-formed nanocontacts: an atomic-scale perspective", *Phys. Chem. Chem. Phys.*, **16**(18), 8201-8222. https://doi.org/10.1039/C3CP54869D

Perdew, J.P., Burke, K. and Ernzerhof, M. (1996), "Generalized gradient approximation made simple", *Phys. Rev. Lett.*, **77**, 3865-3868. https://doi.org/10.1103/PhysRevLett.77.3865

Pinto, N.J. and Gonzalez, R. (2006), "Electrospun hybrid organic/inorganic semiconductor Schottky nanodiode", *Appl. Phys. Lett.*, **89**, 033505. https://doi.org/10.1063/1.2227758

Pomorski, P., Roland, C., Guo, H. and Wang, J. (2003), "First-principles investigation of carbon nanotube capacitance", *Phys. Rev. B*, **67**, 161404(R). https://doi.org/10.1103/PhysRevB.67.161404

Pomorski, P., Pastewka, L., Roland, C., Guo, H. and Wang, J. (2004), "Capacitance, induced charges, and bound states of biased carbon nanotube systems", *Phys. Rev. B*, **69**, 115418. https://doi.org/10.1103/PhysRevB.69.115418

Schönenberger, C., van Houten, H. and Beenakker, C.W.J. (1993), "Polarization charge relaxation and the Coulomb staircase in ultrasmall double-barrier tunnel junctions", *Physica B: Condensed Matter*, **189**(1-4), 218-224. https://doi.org/10.1016/0921-4526(93)90163-Z

Sergeyev, D. (2020a), "Single Electron Transistor Based on Endohedral Metallofullerenes Me@C_{60} (Me = Li, Na, K)", *J. Nano- Electron. Phys.*, **12**(3), 03017. https://doi.org/10.21272/jnep.12(3).03017

Sergeyev, D. (2020b), "Features of the electrical characteristics of an octagraphene nanotube", *J. Nano-Electron. Phys.*, **11**(6), 06022. https://doi.org/10.21272/jnep.11(6).06022

Sergeyev, D. (2020c), "Specific Features of Electron Transport in a Molecular Nanodevice Containing a Nitroamine Redox Center", *Tech. Phys.*, **65**(4), 573-577. https://doi.org/10.1134/S1063784220040180

Sergeyev, D. and Shunkeyev, K. (2018), "Investigation of transport parameters of graphene-based nanostructures", *Russ. Phys. J.*, **60**, 1938-1945. https://doi.org/10.1007/s11182-018-1306-9

Sergeyev, D. and Zhanturina, N. (2019), "Simulation of Electrical Characteristics of Switching Nanostructures "Pt – TiO – Pt" and "Pt – NiO – Pt" with Memory", *Radioengeeniring*, **28**(4), 714-720. https://doi.org/10.13164/re.2019.0714

Smidstrup, S., Stradi, D., Wellendorff, J., Khomyakov, P.A., Vej-Hansen, U.G., Lee, M-E., Ghosh, T., Jonsson, E., Jonsson, H. and Stokbro, K. (2017), "First-principles Green's-function method for surface calculations: A pseudopotential localized basis set approach", *Phys. Rev. B*, **96**, 195309. https://doi.org/10.1103/PhysRevB.96.195309

Smidstrup, S., Markussen, T., Vancraeyveld, P., Wellendorff, J., Schneider, J., Gunst, T., Verstichel, B., Stradi, D., Khomyakov, P.A., Vej-Hansen, U.G. and Lee, M.E. (2020), "QuantumATK: an integrated platform of electronic and atomic-scale modelling tools", *J. Phys.: Condens. Matter.*, **32**, 015901. https://doi.org/10.1088/1361-648X/ab4007

Stokbro, K. (2008), "First-principles modeling of electron transport" *J. Phys.: Condens. Matter.*, **20**, 064216. https://doi.org/10.1088/0953-8984/20/6/064216

Wang, J., Zhou, X., Yang, M., Cao, D., Chen, X. and Shua, H. (2020), "Interface and polarization effects induced Schottky-barrier-free contacts in two-dimensional MXene/GaN heterojunctions", *J. Mater. Chem. C*, **8**, 7350-7357. https://doi.org/10.1039/d0tc01405b

Wu, C.-P., Chen, Y.-H., Hong, Z.-L. and Lin, C.-H. (2018), "Nonlinear vibration analysis of an embedded multi-walled carbon nanotube", *Adv. Nano Res., Int. J.*, **6**(2), 163-182. https://doi.org/10.12989/anr.2018.6.2.163

Xiang, R., Inoue, T., Zheng, Y., Kumamoto, A., Qian, Y., Sato, Y., Liu, M., Tang, D., Gokhale, D., Guo, J. and Hisama, K. (2020), "One-dimensional van der Waals heterostructures", *Science*, **367**(6477), 537-542. https://doi.org/10.1126/science.aaz2570

Yan, Q., Zhou, G., Hao, S., Wu, J. and Duan, W. (2006), "Mechanism of nanoelectronic switch based on telescoping carbon nanotubes", *Appl. Phys. Lett.*, **88**, 173107. http://dx.doi.org/10.1063/1.2198481.

JL